



# Xenobiotica

the fate of foreign compounds in biological systems

ISSN: 0049-8254 (Print) 1366-5928 (Online) Journal homepage: <http://www.tandfonline.com/loi/ixen20>


## Lumiracoxib metabolism in male C57bl/6J mice: characterisation of novel in vivo metabolites

Anthony P. Dickie, Claire E. Wilson, Kay Schreiter, Roland Wehr, Ian D. Wilson & Rob Riley

To cite this article: Anthony P. Dickie, Claire E. Wilson, Kay Schreiter, Roland Wehr, Ian D. Wilson & Rob Riley (2016): Lumiracoxib metabolism in male C57bl/6J mice: characterisation of novel in vivo metabolites, *Xenobiotica*, DOI: [10.1080/00498254.2016.1206239](https://doi.org/10.1080/00498254.2016.1206239)

To link to this article: <http://dx.doi.org/10.1080/00498254.2016.1206239>

 View supplementary material [↗](#)

 Published online: 18 Jul 2016.

 Submit your article to this journal [↗](#)

 Article views: 19

 View related articles [↗](#)

 View Crossmark data [↗](#)

RESEARCH ARTICLE

# Lumiracoxib metabolism in male C57bl/6J mice: characterisation of novel *in vivo* metabolites

Anthony P. Dickie<sup>1</sup>, Claire E. Wilson<sup>1\*</sup>, Kay Schreiter<sup>2</sup>, Roland Wehr<sup>2</sup>, Ian D. Wilson<sup>3</sup>, and Rob Riley<sup>1</sup>

<sup>1</sup>Evotec UK Ltd, Milton Park, Abingdon, UK, <sup>2</sup>Evotec International GmbH, In Vivo Pharmacology, Göttingen, Germany, and <sup>3</sup>Imperial College London, Surgery and Cancer, London

## Abstract

1. The pharmacokinetics and metabolism of lumiracoxib in male C57bl/6J mice were investigated following a single oral dose of 10 mg/kg.
2. Lumiracoxib achieved peak observed concentrations in the blood of  $1.26 \pm 0.51 \mu\text{g/mL}$  0.5 h (0.5–1.0) post-dose with an  $\text{AUC}_{\text{inf}}$  of  $3.48 \pm 1.09 \mu\text{g h/mL}$ . Concentrations of lumiracoxib then declined with a terminal half-life of  $1.54 \pm 0.31$  h.
3. Metabolic profiling showed only the presence of unchanged lumiracoxib in blood by 24 h, while urine, bile and faecal extracts contained, in addition to the unchanged parent drug, large amounts of hydroxylated and conjugated metabolites.
4. No evidence was obtained in the mouse for the production of the downstream products of glutathione conjugation such as mercapturates, suggesting that the metabolism of the drug via quinone–imine generating pathways is not a major route of biotransformation in this species. Acyl glucuronidation appeared absent or a very minor route.
5. While there was significant overlap with reported human metabolites, a number of unique mouse metabolites were detected, particularly taurine conjugates of lumiracoxib and its oxidative metabolites.

## Keywords

Glucuronide conjugation, reactive intermediate, quinone imine, taurine conjugation

## History

Received 5 May 2016  
Revised 21 June 2016  
Accepted 22 June 2016  
Published online 18 July 2016

## Introduction

One of the major causes of drug attrition in the clinic in 2000 was safety, specifically toxicology and clinical safety, accounting for approximately 30% of failures (Kola & Lanhis, 2004). Despite its relatively infrequent occurrence, drug-induced liver injury (DILI) remains the leading cause of acute liver injury in the USA (Chitturi & Farrell, 2011; Kaplowitz, 2005; Senior, 2007) and has resulted in both ‘Black Box’ warnings and drug withdrawals. A major class of drugs associated with DILI is the non-steroidal anti-inflammatory drugs (NSAIDs) which are widely used for the management of joint inflammation and pain associated with osteoarthritis and rheumatoid arthritis. The anti-inflammatory actions of NSAIDs result in part from their inhibition of cyclo-oxygenase (COX-1 and -2), enzymes that catalyse key steps in prostaglandin formation (Marnett et al., 1999; Scott et al., 2004).

Lumiracoxib [2-(2-chloro-6-fluorophenyl)-amino-5-methylbenzeneacetic acid] (Prexige) was developed as a selective COX-2 inhibitor for use in the treatment of

osteoarthritis, rheumatoid arthritis and acute pain and was eventually approved in over 50 countries worldwide (Bannwarth & Berenbaum, 2007; Buvanendran & Barkin, 2007). However, although lumiracoxib was developed relatively recently, and was, therefore, subject to the latest safety evaluation protocols, concerns were nevertheless raised over the clinical safety of the drug after reports of rare, but serious, liver reactions following its use (Li et al., 2008). Thus, DILI, reportedly associated with lumiracoxib administration, has included 14 cases of acute liver failure, two deaths, and three liver transplants (Li et al., 2008). Most cases occurred several months after starting treatment with lumiracoxib, but early presentations were also noted. Many cases involved daily doses exceeding 100 mg, but severe DILI was also reported in those patients who were prescribed 100 mg/day (Singer et al., 2010; Teoh & Farrell, 2003). As a result, since its original approval, lumiracoxib has been withdrawn from the market in a number of countries, mostly due to its potential for causing liver failure, and it is now only available in a few countries, including Mexico, Ecuador and the Dominican Republic (Shi & Klotz, 2008).

The pharmacokinetic (PK) profile of lumiracoxib has been extensively studied in healthy subjects and patients (Mangold et al., 2004; Rordorf et al., 2002; Scott et al., 2004) and the drug has been shown to be absorbed rapidly following oral administration with an absolute bioavailability of

\*Present address: Galderma R&D, Les Templiers, Sophia-Antipolis, France.

Address for correspondence: Mr. Anthony Paul Dickie MChem, Evotec UK Ltd, DMPK, 114 Innovation Drive, Milton Park, Abingdon OX14 4SA, United Kingdom of Great Britain and Northern Ireland. E-mail: anthony.dickie@evotec.com

approximately 74%. A median  $t_{\max}$  is reached in 2 h, and  $C_{\max}$  is proportional to the dose range (25–800 mg). In humans, the drug has a relatively short half-life of 3–6 h, a mean plasma clearance of 8 L/h and a moderate volume of distribution of 9 L as determined following intravenous (i.v.) administration. Lumiracoxib is metabolised predominantly by CYP2C9 with oxidation of the 5-methyl group and hydroxylation of the dihaloaromatic ring as the primary sites of biotransformation (Mangold et al., 2004). Lumiracoxib is structurally similar to diclofenac, another NSAID associated with rare but severe hepatotoxicity in exposed patients (Li et al., 2008). It has been proposed that chemically reactive metabolites may play a role in the mechanism of diclofenac-mediated hepatotoxicity (Boelsterli, 2003; Tang, 2003). By analogy, since lumiracoxib contains a 2'-chloro-6'-fluorophenyl-amino group, the exposed 4'-position on the aromatic ring was predicted to undergo metabolic activation by cytochrome P450 to a reactive quinone–imine intermediate, similar to the mechanism of cytochrome P450 mediated bioactivation of diclofenac (Tang et al., 1999). Bioactivation of lumiracoxib by peroxidases and human liver microsomes gave rise to multiple quinone–imine intermediates and glutathione (GSH) adducts (Tang et al., 1999). The bioactivation of lumiracoxib through quinone–imines may result in GSH depletion, covalent binding to proteins, oxidative stress, eventually leading to the observed hepatotoxicity (Kang et al., 2009). However, this toxicity was not observed in the preclinical species used for the safety evaluation of the drug and, given the clear requirement for reduced attrition in drug development (Kola & Lanhis, 2004), there is an obvious need to develop more predictive models of human metabolism and toxicity including both *in vitro* and *in vivo* model systems. One such *in vivo* model is represented by the recently introduced 'chimeric' humanised mice, where human hepatocytes can replace 90% or more of the murine hepatocytes (Kamimura et al., 2010; Strom et al., 2010). Assuming that the DILI seen in clinical use was the result of hepatic metabolism of lumiracoxib, and also assuming its human metabolic fate is faithfully emulated by such models, the use of chimeric humanised mice might have enabled a more accurate risk assessment for humans. However, prior to studies in chimeric humanised mouse models, it was first necessary to characterise the biotransformation of lumiracoxib in wild-type mice, and compare it with the human metabolic fate of the drug. Here the pharmacokinetics and metabolite profile of lumiracoxib are described over 24 h following oral administration at 10 mg/kg to male C57bl/6J mice.

## Experimental

### Chemicals

Lumiracoxib was purchased from Selleck Chemicals LLC (supplied by Absource Diagnostics GmbH, Munich, Germany) and used as supplied. Acetonitrile and methanol were supplied by Fisher Scientific UK Ltd. (Loughborough, UK). All other chemicals or solvents were purchased from commercial suppliers and were of analytical grade or the best equivalent.

### Animal studies

All animal procedures were performed in accordance with Annex III of the Directive 2010/63/EU applying to

national-specific regulations such as the German law on animal protection. In order to determine pharmacokinetics and the routes, rate of excretion and metabolic fate of lumiracoxib, six male C57bl/6J mice, 8 weeks of age supplied by Charles River Laboratories (Sulzfeld, Germany), were administered by oral gavage either formulation (vehicle control) or lumiracoxib at a nominal dose of 10 mg/kg (a dosing volume of 10 mL/kg) as a solution in water. Mice were housed individually in metabolism cages and for the determination of the pharmacokinetics of lumiracoxib, whole blood (20  $\mu$ L) was collected pre-dose, and 15, 30, 60, 120, 240, 360 and 480 min post-dose from the tail vein into Minivette POCT K-EDTA-coated capillaries and transferred after collection to 96 well plates, pre-prepared with 20  $\mu$ L purified water containing 0.2% v/v phosphoric acid (to stabilise any acyl glucuronide conjugates that might have been present). Urine and faeces for metabolite profiling were collected, over dry ice to ensure sample stability, over 0–8 h and 8–24 h time periods. Urine and faeces from animals that had not been dosed were collected over dry ice over a 24 h period, and used as controls for metabolite identification. Samples were frozen on dry ice and stored at  $-80^{\circ}\text{C}$  until analysis.

After the final sampling time point, the animals were sacrificed by isoflurane inhalation. On termination, the gall bladder was excised and stored at  $-80^{\circ}\text{C}$  until analysis.

### Sample preparation for quantitative analysis

Aliquots of diluted blood (40  $\mu$ L) and diluted blood spiked to provide calibration and QC samples were extracted by the addition of 5 volumes (v/v) of cold acidified acetonitrile containing 200 nM tolbutamide as an internal analysis standard, mixed vigorously and centrifuged (4566 g, 20 min) and diluted 1:3 (v/v) with water. A standard curve was prepared at six concentrations over the range 30–10 000 ng/mL with QC samples at three concentrations over the range 40–4000 ng/mL.

### Quantitative analysis of lumiracoxib in blood

Ultra high-performance liquid chromatography/mass spectrometry (UHPLC-MS/MS), using an unvalidated method, was used to determine blood concentrations of lumiracoxib. Using a CTC HTS-xt PAL autosampler (supplied by AB Sciex UK Ltd, Warrington, UK), 2  $\mu$ L aliquots were injected onto and separated on a BEH C18, 1.7  $\mu$ m, 30  $\times$  2.1 mm column (Waters Ltd, Elstree, UK), maintained at 60  $^{\circ}\text{C}$  within a 1290 thermostatted column compartment (Agilent Technologies Ltd, Stockport, UK) and eluted over 1.3 min using an 1290 binary pump (Agilent Technologies Ltd, Stockport, UK) at an initial flow rate of 1 mL/min. The aqueous mobile phase (solvent A) was water containing 0.1% (v/v) formic acid with acetonitrile containing 0.1% (v/v) formic acid constituting the organic mobile phase (solvent B). The initial mobile phase consisting of 3% solvent B was maintained over 0.1 min, then increased to 22.5% over 0.15 min, then further increased to 77.5% over 0.83 min as the flow rate also increased to 1.5 mL/min. The flow rate finally increased to 1.75 mL/min as solvent B increased to 97% over 0.1 min. This high organic concentration and flow

rate was maintained for 0.1 min before returning to initial conditions for column equilibration for ca. 0.8 min prior to subsequent injections. In order to protect the MS source from contamination the initial 0.3 min of the LC flow was diverted to waste for each injection. Mass spectrometric analyses were conducted on an API 6500 triple quadrupole instrument (AB Sciex UK Ltd, Warrington, UK) fitted with an electrospray ionisation (ESI) source operating in negative ion mode. Detection and quantification of analytes were performed in multiple reaction-monitoring mode (MRM). Compound optimisation was performed using the auto tune algorithm in the DiscoveryQuant Optimise software (AB Sciex UK Ltd, Warrington, UK) capturing declustering potential (DP), entrance potential (EP), collision energy (CE), collision cell exit potential (CXP) and product ion. The optimised transition for lumiracoxib was  $292 > 248$ , with DP  $-8$  V, EP  $-10$  V, CE  $-15$  V and CXP  $-18$  V. Non-optimised transitions corresponding to expected metabolites of lumiracoxib were also analysed simultaneously. The source temperature (TEM) was set to  $700$  °C, IonSpray™ voltage (IS) to  $-4500$  V, curtain gas (CUR) to  $40$  V, ion source gases (GS1 and GS2) to  $60$  V, and collision gas (CAD) to  $7$  V. The instrument was controlled, and data acquired and processed by Analyst™ v.1.6 (AB Sciex UK Ltd, Warrington, UK). Instrument performance (chromatography and response of standards) was assessed before and after sample batch injection to ensure the system was suitable for use.

### Blood lumiracoxib pharmacokinetics

Phoenix WinNonlin 6.4 (Pharsight, Mountain View, CA) was used to produce PK parameters using non-compartmental analysis. Peak (observed) blood concentrations ( $C_{\max}$ ) and  $AUC_{\text{inf}}$ , as determined by the linear trapezoidal rule were determined per animal and presented as the mean ( $n = 3$ ).

### Sample preparation for metabolite profiling and identification

In addition to blood samples obtained for PK analysis as described above, aliquots of diluted blood ( $40 \mu\text{L}$ ) obtained from animals pre-dose and 24 h post-dose were extracted by the addition of 4 volumes (v/v) of acetonitrile, mixed vigorously and centrifuged ( $4566$  g, 20 min) and diluted 1:2 (v/v) with water.

Urine samples obtained from both dosed and control animals were pooled by dose group according to weight of urine collected, for each time range (0–8 h and 8–24 h). Pooled urine samples were centrifuged ( $20\,800$  g, 5 min) to remove particulates.

Gall bladders removed at 24 h from dosed animals were extracted with 8 volumes (w/v) of acetonitrile, mixed vigorously and sonicated for 30 min. The bile extract supernatants were pooled by dose group according to weight of gall bladder, centrifuged ( $20\,800$  g, 5 min) to remove particulates and diluted 1:2 (v/v) with water.

Faeces samples obtained from both dosed and control animals were extracted first with 6 volumes (w/v) of MeOH:H<sub>2</sub>O 1:1 (v/v) and centrifuged ( $4566$  g, 20 min). The supernatant was removed and the pellet resuspended in three volumes (w/v) of MeOH, and after removal of solid matter by

centrifugation ( $4566$  g, 20 min) the supernatants were pooled by dose group according to weight of faeces collected, for each time range (0–8 h and 8–24 h). The combined supernatants were evaporated to ca.  $100 \mu\text{L}$  under a stream of dry nitrogen at ambient temperature.

### Metabolite profiling and identification

High-performance liquid chromatography/quadrupole time-of-flight mass spectrometry (HPLC-QTOF-MS/MS) was used to identify metabolites present in extracts of mouse blood, faeces, bile and urine samples.

Using a 2777 CTC HTS-xt PAL autosampler (supplied by Waters Ltd, Elstree, UK),  $50 \mu\text{L}$  aliquots were injected onto and separated on a Hypersil Gold C18,  $5 \mu\text{m}$ ,  $250 \times 4.6$  mm column (Fisher Scientific UK Ltd, Loughborough, UK) with a SecurityGuard C18,  $3 \mu\text{m}$  pre-column filter (Phenomenex Inc., Macclesfield, UK), all maintained at  $30$  °C within a Grace 7956R column heater/chiller (Hichrom Ltd, Theale, UK) and eluted over 60 min using an Acquity UPLC binary pump (Waters Ltd, Elstree, UK) at a flow rate of  $1$  mL/min. The aqueous mobile phase (solvent A) was  $10$  mM ammonium acetate (unadjusted, ca. pH 7) with acetonitrile constituting the organic mobile phase (solvent B). This chromatographic method had been developed previously to resolve diclofenac and its metabolites (Sarda et al., 2012). The initial mobile phase consisted of 5% solvent B, which was increased to 14% over a period of 4 min, then further increased to 34% in 41 min, and to 45% over 5 min before finally increasing to 95% over 0.1 min. This high organic concentration was maintained for 5 min before returning to 5% solvent B for column equilibration for 5 min prior to subsequent injections. The post-column eluent passed through a photo-diode array detector (Waters Ltd, Elstree, UK) set at a variable wavelength of 210–400 nm at 20 spectra/s, before entering the mass spectrometer. Mass spectrometric analyses were conducted on a Xevo G2 Q-ToF instrument (Waters Ltd, Wilmslow, UK) fitted with an electrospray ionisation (ESI) source operating in positive ion mode. The capillary voltage was set to  $+500$  V, sampling cone to  $25$  V and extraction cone to  $4$  V. The source temperature was set to  $150$  °C, desolvation temperature to  $500$  °C, the cone gas flow was set to  $50$  L/h, and the desolvation gas flow to  $1000$  L/h. Mass spectrometric data were collected in resolution mode, in centroid data format, with a scan time of 1 s and a scan range of 50–1200 Th at a nominal resolution of 30 000. Full scan and product ion mass spectra were acquired simultaneously by HPLC-QTOF-MS<sup>E</sup>. Collision energy was applied over a ramp of 20–40 eV for each product ion scan. The instrument was controlled and data acquired by MassLynx™ v.4.1 (Waters Ltd, Wilmslow, UK). Full scan and product ion mass spectra were interrogated by extracting chromatograms of potential metabolites using MassLynx™ v.4.1 from the raw data. Comparison was also made with samples from the control group or taken pre-dose to minimise the potential for false positives from endogenous compounds.

The mass spectrometer was calibrated with a solution of  $5$  mM sodium formate in positive ion mode according to the instructions of the manufacturer, and further aligned with an internal lock mass of  $2$  ng/ $\mu\text{L}$  leucine-enkephalin ( $[M + H]^+ 556.2771$  Th) infused at  $10 \mu\text{L}/\text{min}$  and scanned for

1 s every 57 s. Instrument performance (chromatography, response and mass accuracy of standards) was assessed before and after sample batch injection to ensure the system was suitable for use. The measured mass accuracy for standards was less than 5 ppm.

## Results and discussion

### Pharmacokinetics of lumiracoxib

The blood concentration versus time profiles for lumiracoxib in the three wild-type C57bl/6J mice ( $n=3$ ) are shown in Figure 1. After administration of a single oral dose (10 mg/kg) lumiracoxib was rapidly absorbed, with mean peak blood concentrations of  $1.26 \pm 0.51 \mu\text{g/mL}$  being reached at approximately 0.5 h (0.5–1.0) post-dose. Good, but variable, exposure was achieved with the mean  $\text{AUC}_{\text{inf}}$  determined as  $3.48 \pm 1.09 \mu\text{g h/mL}$  and an apparent mean terminal half-life of  $1.54 \pm 0.31$  h. By way of comparison with healthy human volunteers ( $n=4$ ), when lumiracoxib was administered as a single 400 mg dose (ca. 5 mg/kg), peak plasma concentrations were achieved at ca. 4 h post-dose with an apparent mean terminal half-life of ca. 6.54 h (Mangold et al., 2004). The PK properties of [ $^{14}\text{C}$ ]-lumiracoxib in healthy male subjects (Mangold et al., 2004) are compared with those generated in C57bl/6J mice in the present study in Table 1.

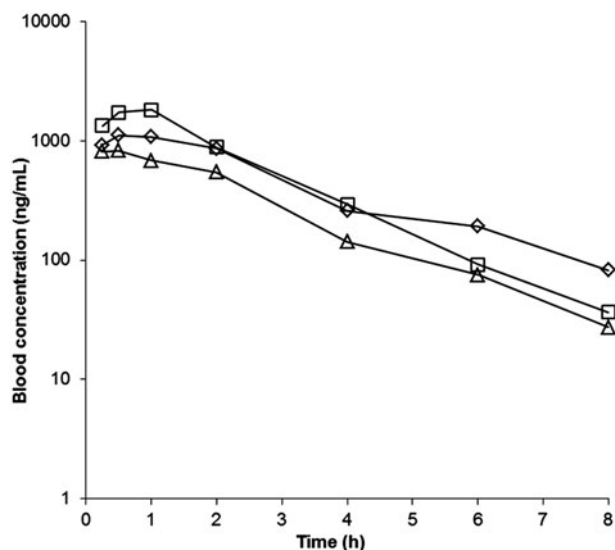


Figure 1. Blood concentration–time profiles for lumiracoxib following single oral administration at 10 mg/kg to male C57bl/6J mice. Symbols represent concentration–time profiles from individual animals.

Table 1. Pharmacokinetic parameters for [ $^{14}\text{C}$ ]-lumiracoxib in the plasma of healthy male subjects and lumiracoxib in the blood of C57bl/6J mice.

	Plasma healthy male subjects	Blood C57bl/6J mice
Dose (mg/kg)	5.09 <sup>a</sup>	10
$C_{\text{max}}$ ( $\mu\text{g/mL}$ )	$7.28 \pm 1.39$	$1.26 \pm 0.51$
$t_{\text{max}}$ (h)	4.0 (2.5–4.0)	0.5 (0.5–1.0)
$\text{AUC}_{\text{inf}}$ ( $\mu\text{g h/mL}$ )	$48.4 \pm 6.12$	$3.48 \pm 1.09$
$t_{1/2}$ (h)	$6.54 \pm 1.43$	$1.54 \pm 0.31$

Values are mean  $\pm$  SD, except for  $t_{\text{max}}$  which are median (range).

<sup>a</sup>Four subjects received a single 400-mg oral dose of [ $^{14}\text{C}$ ]-lumiracoxib. Using the mean weight of the subjects ( $78.6 \pm 8.8$  kg), the dose can be calculated as 5.09 mg/kg (Mangold et al., 2004).

### Blood metabolite profiles of lumiracoxib

The only drug-related compound detected in the blood of these animals at 24 h post-dose was lumiracoxib itself in trace quantities.

### Urinary metabolite profiles of lumiracoxib

Clearly, in the absence of authentic metabolite standards (or radiolabelled drug), it is not possible to discuss the metabolic fate of lumiracoxib in the mouse based on quantitative data as the relative MS responses of the metabolites compared with lumiracoxib are not known.

The qualitative HPLC-QTOF-MS profiles observed for the 0–8 and 8–24 h urine samples (Figure 2a and b) showed the presence of unchanged lumiracoxib (*P*) and a number of oxidised and conjugated metabolites. The chromatographic peak observed at a retention time of 43.8 min was consistent with the presence of unchanged drug (an authentic lumiracoxib standard eluted at 44.2 min). The putative lumiracoxib peak was characterised by a protonated molecular ion  $[\text{M} + \text{H}]^+$  whose predominant  $^{35}\text{Cl}/^{12}\text{C}$  isotope was detected at a mass/charge ( $m/z$ ) of 294.0695 (Figure 4a). This is in close agreement ( $\Delta m = +0.3$  mDa or 1.0 ppm) with the theoretical  $m/z$  of 294.0692 for lumiracoxib's protonated empirical formula  $\text{C}_{15}\text{H}_{14}\text{N}_1\text{O}_2\text{Cl}_1\text{F}_1$ . High-energy mass spectra from the  $\text{MS}^E$  experiment afforded product ions via an apparently relatively facile loss of  $\text{CO}_2/\text{H}_2$  ( $m/z$  248) and subsequent loss of either HF ( $m/z$  228) or HCl ( $m/z$  212). Radical cations associated with mono-electronic cleavage of the carbon–halogen bonds ( $m/z$  229 and 213) were also seen following loss of F or Cl radicals, respectively. Loss of  $\text{CH}_2$  from  $m/z$  212 resulted in an ion with  $m/z$  198, and ultimate product ions were detected that are postulated to correspond to the N-linked bi-aryl ring system ( $m/z$  169) and fluorophenyl ( $m/z$  95) cations (Figure 4a). A proposed fragmentation scheme for lumiracoxib is provided in Supplementary Figure S1.

The metabolite profile for the 8–24 h urinary sampling time point was dominated by the chromatographic peak (**M9**) eluting at 30.8 min. This peak contained a protonated molecular ion  $[\text{M} + \text{H}]^+$  detected at  $m/z$  310.0639 (Figure 4b). This matches well ( $\Delta m = -0.2$  mDa or 0.6 ppm) with the expected composition of a mono-hydroxylated metabolite with protonated empirical formula  $\text{C}_{15}\text{H}_{14}\text{N}_1\text{O}_3\text{Cl}_1\text{F}_1$  (theoretical  $m/z$  310.0641). High-energy mass spectra gave product ions consistent with hydroxylation of the halogenated ring ( $m/z$  264, 244, 228 and 214) corresponding with the addition of a single oxygen atom to those described above for lumiracoxib ( $m/z$  248, 228, 212 and 198). The position of hydroxylation in the ring could not be definitively assigned in the absence of an authentic standard, however, since hydroxylation at the 4' position has been described for lumiracoxib in human (Mangold et al., 2004) and for diclofenac in mouse (Sarda et al., 2012), it therefore seems reasonable to assume that for lumiracoxib in mouse the predominant ring hydroxylation has taken place at the 4' position. The same product ions ( $m/z$  264, 244 and 228) were detected within a chromatographic peak (**M1**), observed eluting with a retention time of 8.9 min, which contained a protonated molecular ion  $[\text{M} + \text{H}]^+$  at  $m/z$  486.0959 (Figure 4c). This is in good agreement

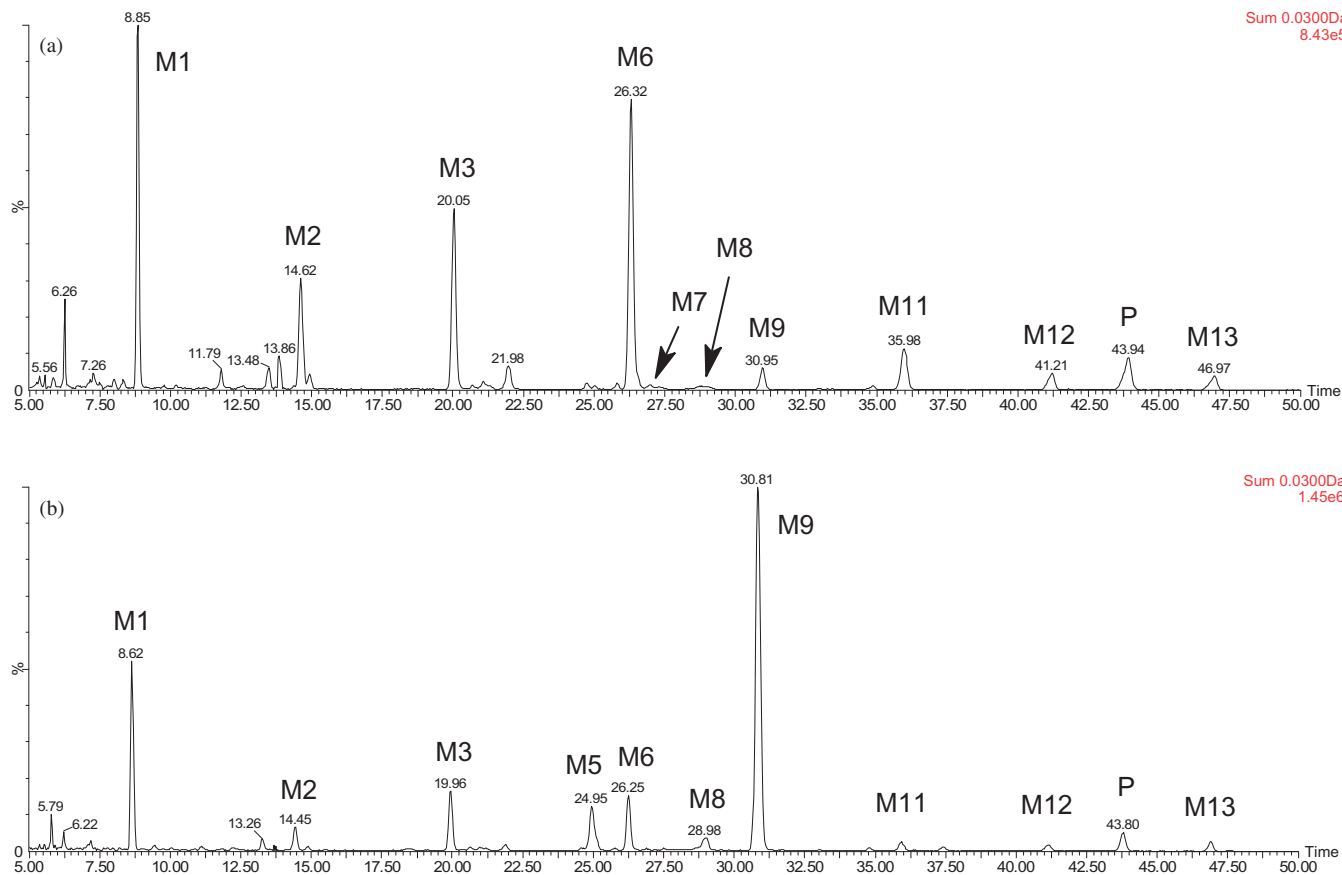


Figure 2. HPLC-QTOF-MS profiles of lumiracoxib and its most abundant metabolites in urine (a) 0–8 h and (b) 8–24 h following single oral administration of 10 mg/kg lumiracoxib to male C57bl/6J mice.

( $\Delta m = -0.3$  mDa or 0.6 ppm) with a hydroxylated and glucuronidated metabolite with a protonated empirical formula  $C_{21}H_{22}N_1O_9Cl_1F_1$  (theoretical  $m/z$  486.0962). Due to its early retention time and the similar fragmentation pattern, this metabolite is postulated to be the ether glucuronide conjugate of 4'-hydroxylumiracoxib. A further metabolite peak (**M13**) observed eluting after lumiracoxib itself at 46.9 min had an  $m/z$  of 401.0729 consistent with a protonated molecular ion  $[M+H]^+$  and an empirical formula of  $C_{17}H_{19}N_2O_4Cl_1F_1S_1$  (theoretical  $m/z$  401.0733,  $\Delta m = -0.4$  mDa or 1.0 ppm). This corresponds to the composition of a taurine conjugation at the carboxylic acid moiety. High-energy mass spectra afforded product ions similar to those of lumiracoxib ( $m/z$  248 and 212), and a discrete fragment with  $m/z$  276 corresponding with loss of taurine via cleavage at the carbonyl (Figure 4d). In addition to these metabolites, ions consistent with the presence of the 4',5-dihydroxylated lumiracoxib (**M2**), an unassigned hydroxylated and taurine conjugated metabolite (**M3**), a 5-hydroxylactam (**M5**), 5-hydroxylumiracoxib produced *via* oxidative metabolism of the methyl group (**M6**), a glucuronidated 5-hydroxylactam (**M7**) and a glucuronidated 4'-hydroxylactam (**M8**), a taurine conjugate of 4' or 5-hydroxylated lumiracoxib (**M10**), an unassigned hydroxylactam (**M11**) and a benzyl taurine (**M12**) were also detected (Table 2). As can be seen from the extracted mass chromatograms (Figure 2a and b), the 0–8 and 8–24 h urine samples both contained a qualitatively similar array of metabolites. However, based on the signal response, the 0–8 h profile was composed mainly of metabolites **M1**, **2**, **3** and **6**, while the

8–24 h samples were dominated by the 4'-hydroxy- and 4'-hydroxyglucuronide.

### Faecal metabolite profiles of lumiracoxib

As in urine, a complex metabolic profile for lumiracoxib was observed in faecal extracts. The HPLC-QTOF-MS profiles for 0–8 h and 8–24 h were dominated by the presence of the 4'-hydroxy metabolite (**M9**) (Figure 3a and b). Two lumiracoxib metabolites featured in the faecal profiles that were not observed in urine samples, specifically **M4**, eluting at 21.2 min which corresponded to the methyl group oxidised carboxylic acid ( $m/z$  324.0445,  $C_{15}H_{12}N_1O_4Cl_1F_1$ ) and another chromatographic peak (**M10**) observed at 34.9 min. This metabolite had an  $m/z$  of 417.0687 (Figure 3a and b) consistent with a protonated molecular ion  $[M+H]^+$  with an empirical formula of  $C_{17}H_{19}N_2O_5Cl_1F_1S_1$  (theoretical  $m/z$  417.0682,  $\Delta m = +0.5$  mDa or 1.2 ppm) corresponding to the composition of a hydroxylated metabolite of the drug that had been further metabolised to a taurine conjugate *via* the carboxylic acid moiety.

Prominent peaks were also noted for the 5-hydroxy metabolite and its cyclised lactam equivalent, plus further oxidation to 5-carboxy and 4',5-dihydroxy metabolites, together with unchanged lumiracoxib. Relatively smaller signals were detected for the direct taurine conjugate of lumiracoxib, the side chain shortened benzyl taurine and an unassigned hydroxytaurine conjugate. When the bile sample collected 24 h after dosing was examined, no metabolites were observed and only traces of unchanged lumiracoxib were

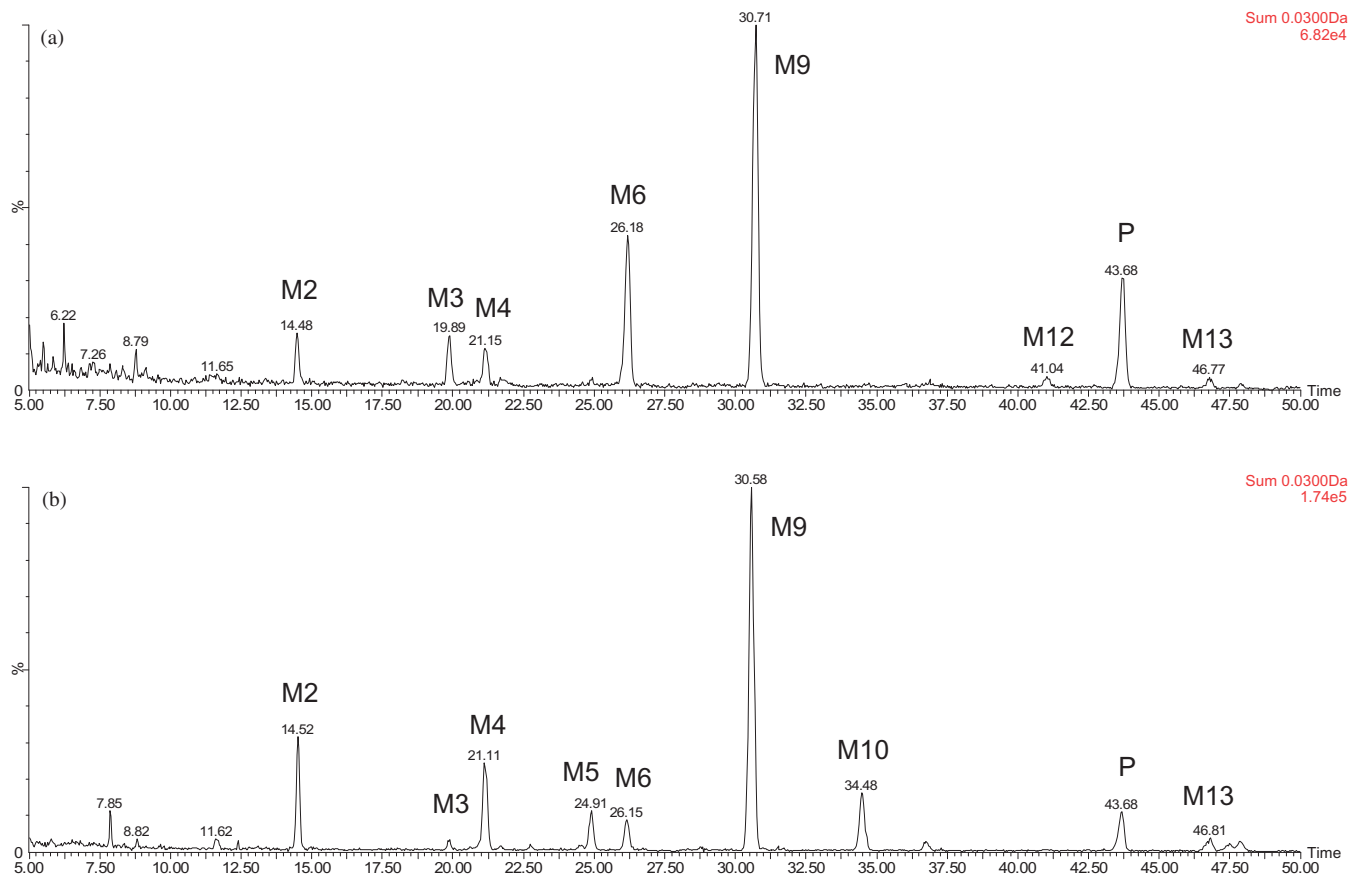


Figure 3. HPLC-QTOF-MS profiles of lumiracoxib and its most abundant metabolites in faeces (a) 0–8 h and (b) 8–24 h following single oral administration of 10 mg/kg lumiracoxib to male C57bl/6J mice.

Table 2. Summary of HPLC and mass spectrometric data obtained for lumiracoxib and its metabolites in mouse urine, faeces, bile and blood.

Peak ID	$t_R$ (min)	Assignment	Elemental composition [M + H] <sup>+</sup>	Theoretical $m/z$ ( <sup>35</sup> Cl/ <sup>12</sup> C isotope [M + H] <sup>+</sup> )	Observed $m/z$ ( <sup>35</sup> Cl/ <sup>12</sup> C isotope [M + H] <sup>+</sup> )	$\Delta m$ (observed-theoretical $m/z$ ) (mDa)
<b>P</b>	<b>43.9</b>	<b>Lumiracoxib</b>	<b>C<sub>15</sub>H<sub>14</sub>N<sub>1</sub>O<sub>2</sub>Cl<sub>1</sub>F<sub>1</sub></b>	<b>294.0692</b>	<b>294.0695</b>	<b>+0.3</b>
M1	8.9	4'-OH glucuronide	C <sub>21</sub> H <sub>22</sub> N <sub>1</sub> O <sub>9</sub> Cl <sub>1</sub> F <sub>1</sub>	486.0962	486.0959	-0.3
N/A	N/A	5-COOH, glucuronide				
N/A	N/A	5-COOH, 4'-OH sulphate				
N/A	N/A	5-COOH lactam, 4'-OH sulphate				
N/A	N/A	4'-OH, 5-COOH				
<b>M2</b>	<b>14.6</b>	<b>4',5 dihydroxy</b>	<b>C<sub>15</sub>H<sub>14</sub>N<sub>1</sub>O<sub>4</sub>Cl<sub>1</sub>F<sub>1</sub></b>	<b>326.0590</b>	<b>326.0590</b>	<b>0.0</b>
N/A	N/A	4'-OH, 5-COOH lactam				
M3	20.2	Unassigned OH taurine	N/A	N/A	N/A	N/A
<b>M4</b>	<b>21.1</b>	<b>5-COOH</b>	<b>C<sub>15</sub>H<sub>12</sub>N<sub>1</sub>O<sub>4</sub>Cl<sub>1</sub>F<sub>1</sub></b>	<b>324.0433</b>	<b>324.0445</b>	<b>+1.2</b>
N/A	N/A	4'-OH, 5-COOH lactam, glucuronide				
N/A	N/A	5-COOH lactam				
N/A	N/A	4'-OH, 5-COOH lactam, unassigned OH				
N/A	N/A	4'-OH, 5-COOH lactam, unassigned OH glucuronide				
N/A	N/A	5-COOH lactam, glucuronide				
M5	25.0	5-OH lactam	C <sub>15</sub> H <sub>12</sub> N <sub>1</sub> O <sub>2</sub> Cl <sub>1</sub> F <sub>1</sub>	292.0535	292.0540	+0.5
<b>M6</b>	<b>26.3</b>	<b>5-OH</b>	<b>C<sub>15</sub>H<sub>14</sub>N<sub>1</sub>O<sub>3</sub>Cl<sub>1</sub>F<sub>1</sub></b>	<b>310.0641</b>	<b>310.0644</b>	<b>+0.3</b>
<b>M7</b>	<b>26.5</b>	<b>5-OH lactam glucuronide</b>	<b>C<sub>21</sub>H<sub>20</sub>N<sub>1</sub>O<sub>8</sub>Cl<sub>1</sub>F<sub>1</sub></b>	<b>468.0856</b>	<b>468.0854</b>	<b>-0.2</b>
<b>M8</b>	<b>29.0</b>	<b>4'-OH lactam glucuronide</b>	<b>C<sub>21</sub>H<sub>20</sub>N<sub>1</sub>O<sub>8</sub>Cl<sub>1</sub>F<sub>1</sub></b>	<b>468.0856</b>	<b>468.0856</b>	<b>0.0</b>
<b>M9</b>	<b>31.0</b>	<b>4'-OH</b>	<b>C<sub>15</sub>H<sub>14</sub>N<sub>1</sub>O<sub>3</sub>Cl<sub>1</sub>F<sub>1</sub></b>	<b>310.0641</b>	<b>310.0639</b>	<b>-0.2</b>
M10	34.9	4'-OH or 5-OH taurine	C <sub>17</sub> H <sub>19</sub> N <sub>2</sub> O <sub>5</sub> Cl <sub>1</sub> F <sub>1</sub> S <sub>1</sub>	417.0682	417.0687	+0.5
M11	36.0	Unassigned OH lactam	C <sub>15</sub> H <sub>12</sub> N <sub>1</sub> O <sub>2</sub> Cl <sub>1</sub> F <sub>1</sub>	292.0535	292.0540	+0.5
M12	41.2	Benzyl, taurine	C <sub>16</sub> H <sub>17</sub> N <sub>2</sub> O <sub>4</sub> Cl <sub>1</sub> F <sub>1</sub> S <sub>1</sub>	387.0576	387.0573	-0.3
M13	46.9	Taurine	C <sub>17</sub> H <sub>19</sub> N <sub>2</sub> O <sub>4</sub> Cl <sub>1</sub> F <sub>1</sub> S <sub>1</sub>	401.0733	401.0729	-0.4

Bold text corresponds to the parent or metabolites seen in both humans (Mangold et al., 2004) and mice. Standard text corresponds to metabolites seen only in mice. Italicized text corresponds to metabolites seen only in humans (Mangold et al., 2004).

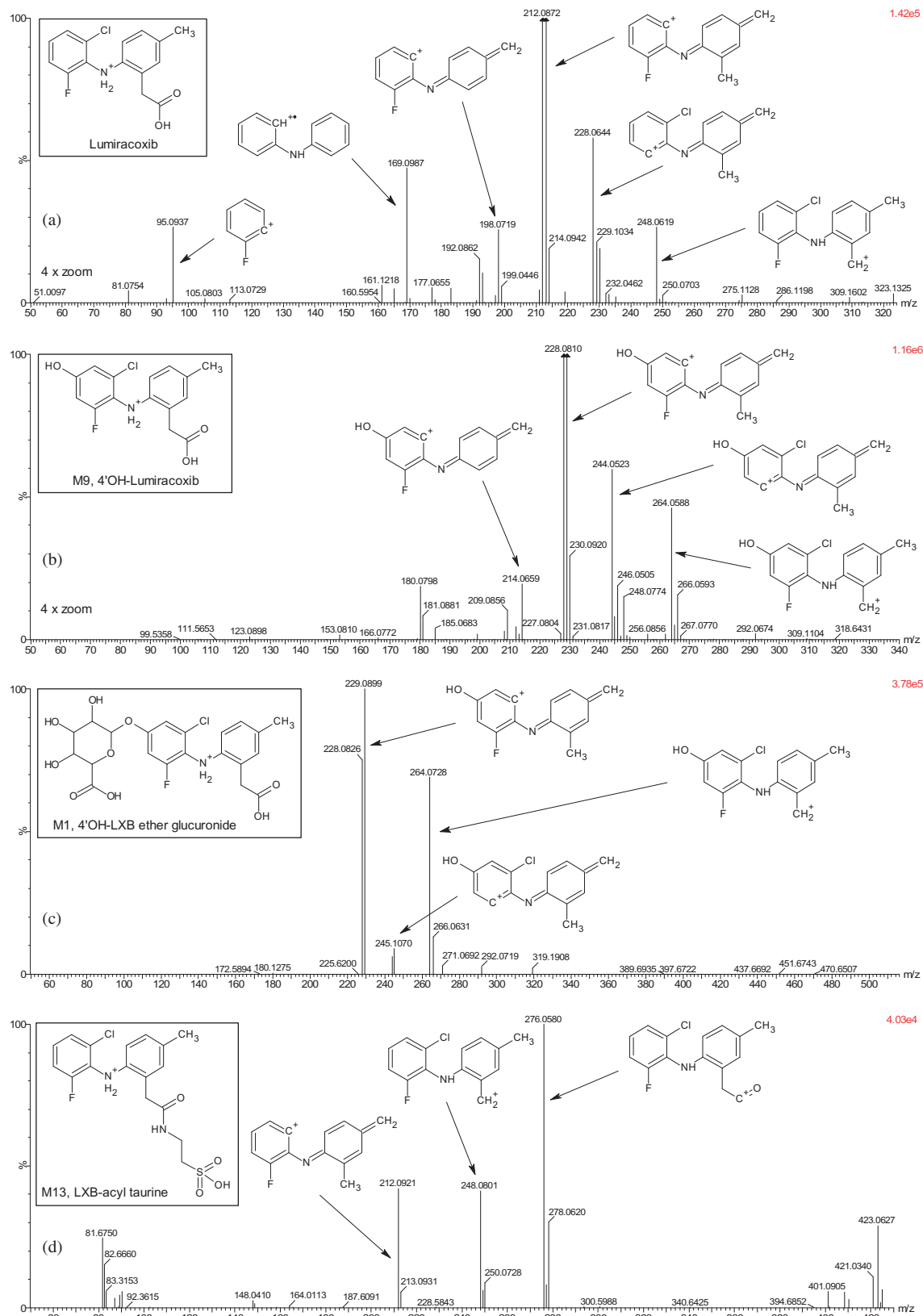


Figure 4. Representative product ion spectra of (a) lumiracoxib and selected murine metabolites (b) 4'-hydroxy, (c) 4'-hydroxy glucuronide and (d) taurine conjugate. In spectra (a) and (b), the y-axis has been zoomed in four times to scale for the intensity of the dominant  $m/z$  212/228 product ion obtained from fragmentation of lumiracoxib and its 4'-hydroxy metabolite, respectively.

detected, indicating that by this time point, the drug had been largely eliminated. These results are summarised in Table 2, and illustrated in Figure 3(a and b) (corresponding to the 0–8 h and 8–24 h faecal metabolite profiles, respectively). In

addition to the spectral data provided in Figure 4, further representative extracted ion spectra of lumiracoxib and selected murine metabolites are provided in Supplementary information (Figure S2).



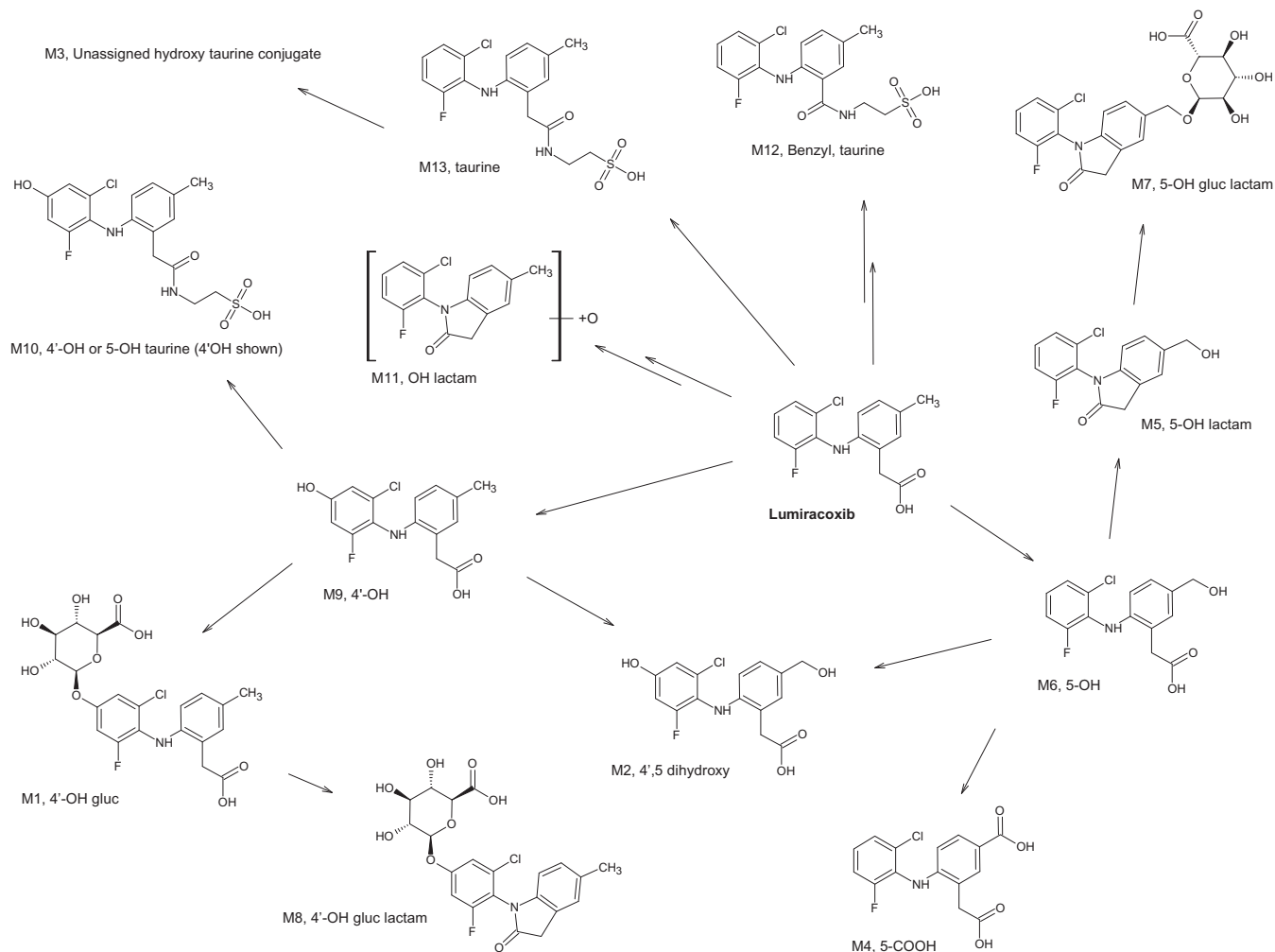


Figure 5. Proposed metabolic pathway of lumiracoxib in C57bl/6J mouse. Double arrows indicate a multi-stage metabolic process to arrive at the detected metabolite.

Overall the results presented here reveal the metabolic fate of lumiracoxib in the mouse to be complex (summarised in Figure 5). Oxidative biotransformations were observed in the C57bl/6J mouse, with aromatic hydroxylation at the 4' position (**M9**) and aliphatic hydroxylation of the ring methyl group (**M6**), followed by further oxidation to the carboxylic acid (**M4**). In the case of the 4' metabolite, ether glucuronidation to **M1** was also seen. These metabolites were also detected in studies in human subjects. However, significant species differences in metabolism were seen with e.g. **M3**, **M4**, **M5**, **M7**, **M8** and **M10–M13** apparently unique to the mouse. These metabolites include a number of taurine conjugates (**M3**, **M10**, **M12** and **M13**) one of which (**M12**) corresponded to a side-chain shortened benzyl-taurine conjugate (see Table 2 and Figure 5). The metabolism of lumiracoxib in the mouse thus has a number of parallels to that of diclofenac, with which it shares many structural similarities (Sarda et al., 2012). However, differences between the metabolism of lumiracoxib in humans and mice are apparent, particularly with respect to the absence of 5-hydroxysulphates, and the number and variety of lactams containing the carboxylic acid produced *via* oxidation of the 5-methyl group (see Table 2).

Both diclofenac and lumiracoxib are known human hepatotoxins, and indeed the rare but serious hepatotoxicity

caused by the latter resulted in its withdrawal from therapeutic use. In the case of diclofenac the mechanism of the observed hepatotoxicity has been proposed as being the result of the production of chemically reactive metabolites (Boelsterli, 2003; Poon et al., 2001; Tang, 2003; Waldon et al., 2010) via CYP450-catalyzed hydroxylation at the 4'- and 5-positions and subsequent formation of highly reactive quinone-imine intermediates (although reactive acyl glucuronides have also been suggested as a toxic intermediate). Evidence for the production of quinone imines from reactive metabolites of lumiracoxib was provided by the detection of two novel mercapturates *in vitro* (Li et al., 2008). Thus, although the methyl substituent inserted into lumiracoxib structure effectively blocks the vulnerable 5-position present in diclofenac as a site for aromatic hydroxylation, the 4'-position remains available for bio activation through hydroxylation and subsequent quinone-imine formation. This metabolic activation was shown to be CYP2C-mediated in *in vitro* studies (Li et al., 2008) employing both rat and human liver microsomes and human hepatocytes preparations. The metabolites were identified as the N-acetylcysteine (NAC) conjugates, 3'-NAC-4'-hydroxy lumiracoxib and 4'-hydroxy-6'-NAC-des-fluoro lumiracoxib. Interestingly, an analogous metabolic dehalogenation, with the production of a glutathione conjugate, 4'-hydroxy-2'-glutathion-deschloro-diclofenac, has also

been seen on incubation of diclofenac with human liver microsomes (Yu et al., 2005). However, neither of the two mercapturates (or any related glutathione-related metabolites) was reported for studies in humans (e.g. Mangold et al., 2004) and, despite careful searching of the acquired LC-MS data, there was no trace of these metabolites in the excreta obtained from the mice in this study.

## Conclusions

Examination of the metabolic fate of lumiracoxib in the male C57bl/6J mouse has revealed a complex metabolic fate for the compound, dominated by oxidative metabolism (aromatic ring oxidation at the 4' position and hydroxylation of the 5-methyl group) and conjugation of these hydroxylated metabolites, and indeed lumiracoxib itself, with taurine or glucuronic acid. Acyl glucuronidation appeared to be either absent or a very minor route; however, ether glucuronidation of hydroxylated metabolites appeared quantitatively important. The metabolism of lumiracoxib in the mouse at this dose failed to reveal the presence of glutathione conjugates or metabolic dehalogenation that could potentially be associated with hepatotoxicity observed in humans. In the case of lumiracoxib, based on the differences in metabolic profiles obtained for mice and those reported for humans, the mouse (despite some similarities) may not represent a good model for man.

## Declaration of interest

The authors report no that they have no conflicts of interest.

## References

- Bannwarth B, Berenbaum F. (2007). Lumiracoxib in the management of osteoarthritis and acute pain. *Expert Opin Pharmacother* 8:1551–64.
- Boelsterli UA. (2003). Diclofenac-induced liver injury: a paradigm of idiosyncratic drug toxicity. *Toxicol Appl Pharmacol* 192:307–22.
- Buvanendran A, Barkin R. (2007). Lumiracoxib. *Drugs Today* 43: 137–47.
- Chitturi S, Farrell GC. (2011). Identifying who is at risk of drug-induced liver injury: is human leukocyte antigen specificity the key? *Hepatology* 53:358–62.
- Kamimura H, Nakada N, Suzuki K, et al. (2010). Assessment of chimeric mice with humanized liver as a tool for predicting circulating human metabolites. *Drug Metab Pharmacokinet* 25:223–35.
- Kang P, Dalvie D, Smith E, Renner M. (2009). Bioactivation of lumiracoxib by peroxidases and human liver microsomes: identification of multiple quinone imine intermediates and GSH adducts. *Chem Res Toxicol* 22:106–17.
- Kola I, Lanhis J. (2004). Can the pharmaceutical industry reduce attrition rates? *Nat Rev Drug Discov* 3:711–16.
- Kaplowitz N. (2005). Idiosyncratic drug hepatotoxicity. *Nat Rev Drug Discov* 4:489–99.
- Li Y, Slatte JG, Zhang Z, et al. (2008). *In vitro* metabolic activation of lumiracoxib in rat and human liver preparations. *Drug Metab Dispos* 36:469–73.
- Mangold JB, Gu H, Rodriguez LC, et al. (2004). Pharmacokinetics and metabolism of lumiracoxib in healthy male subjects. *Drug Metab Dispos* 32:566–71.
- Marnett LJ, Rowlinson SW, Goodwin DC, et al. (1999). Arachidonic acid oxygenation by COX-1 and COX-2. Mechanisms of catalysis and inhibition. *J Biol Chem* 274:22903–6.
- Poon GK, Chen Q, Teffera Y, et al. (2001). Bioactivation of diclofenac via benzoquinone imine intermediates-identification of urinary mercapturic acid derivatives in rats and humans. *Drug Metab Dispos* 29:1608–13.
- Rordorf C, Scott G, Milosavljev S, et al. (2002). Steady state pharmacokinetics, pharmacodynamics, safety and tolerability of COX189 in healthy subjects. *Ann Rheum Dis* 61:420. Abstract AB0284.
- Sarda S, Page C, Pickup K, et al. (2012). Diclofenac metabolism in the mouse: novel *in vivo* metabolites identified by high performance liquid chromatography coupled to linear ion trap mass spectrometry. *Xenobiotica* 42:179–94.
- Scott G, Rordorf C, Reynolds C, et al. (2004). Pharmacokinetics of lumiracoxib in plasma and synovial fluid. *Clin Pharmacokinet* 43: 467–78.
- Senior JR. (2007). Drug hepatotoxicity from a regulatory perspective. *Clin Liver Dis* 11:507–24.
- Shi S, Klotz U. (2008). Clinical use and pharmacological properties of selective COX-2 inhibitors. *Eur J Clin Pharmacol* 64:233–52.
- Singer JB, Lewitzky S, Leroy E, et al. (2010). A genome-wide study identifies HLA alleles associated with lumiracoxib-related liver injury. *Nat Genet* 42:711–14.
- Strom SC, Davila J, Grompe M. (2010). Chimeric mice with humanized liver: tools for the study of drug metabolism, excretion, and toxicity. *Methods Mol Biol* 640:491–509.
- Tang W. (2003). The metabolism of diclofenac-enzymology and toxicology perspectives. *Curr Drug Metab* 4:319–29.
- Tang W, Stearns RA, Bandiera SM, et al. (1999). Studies on cytochrome P-450-mediated bioactivation of diclofenac in rats and in human hepatocytes: identification of glutathione conjugated metabolites. *Drug Metab Dispos* 27:365–72.
- Teoh NC, Farrell GC. (2003). Hepatotoxicity associated with non-steroidal anti-inflammatory drugs. *Clin Liver Dis* 7:401–13.
- Waldon DJ, Teffera Y, Colletti AE, et al. (2010). Identification of quinone imine containing glutathione conjugates of diclofenac in rat bile. *Chem Res Toxicol* 23:1947–53.
- Yu LJ, Chen Y, De Ninno MP, et al. (2005). Identification of a novel glutathione adduct of diclofenac, 4'-hydroxy-2'-glutathion-deschloro-diclofenac, upon incubation with human liver microsomes. *Drug Metab Dispos* 33:484–8.

Supplementary material available online